

Semester Thesis

Sensing and characterization of the motor dynamics on an omnidirectional flying vehicle

Spring Term 2020

Declaration of originality

The signed declaration of originality is a component of every semester paper, Bachelor's thesis, Master's thesis and any other degree paper undertaken during the course of studies, including the respective electronic versions.

Lecturers may also require a declaration of originality for other written papers compiled for their courses.

I hereby confirm that I am the sole author of the written work here enclosed and that I have compiled it in my own words. Parts excepted are corrections of form and content by the supervisor.

Title of work (in block letters):

Sensing and characterization of the motor dynamics on an omnidirectional flying vehicle

Authored by (in block letters):

For papers written by groups the names of all authors are required.

Name(s):

Tapia Benavides

First name(s):

Fausto

With my signature I confirm that

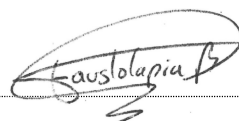
- I have committed none of the forms of plagiarism described in the '[Citation etiquette](#)' information sheet.
- I have documented all methods, data and processes truthfully.
- I have not manipulated any data.
- I have mentioned all persons who were significant facilitators of the work.

I am aware that the work may be screened electronically for plagiarism.

Place, date

20.07.2020

Signature(s)



For papers written by groups the names of all authors are required. Their signatures collectively guarantee the entire content of the written paper.

Contents

Abstract	iv
Symbols	v
1 Introduction	1
2 Literature Review	3
2.1 Brush-less DC motor driving	3
2.1.1 Brush-less DC motor	3
2.1.2 BLDC motor driving methods	3
2.2 Electronic Speed Controllers	5
2.2.1 General structure	5
2.2.2 Communications	5
2.3 Related Work on ESCs characterization	8
2.3.1 Efficiency	8
2.3.2 Modeling for Control	8
3 Experimental Setup	10
3.1 Equipment	10
3.1.1 ESC Assessment	10
3.1.2 Overall setup	11
3.2 Software toolboxes	12
3.3 Software developed	12
4 ESC charaterization	13
5 Conclusions and Recommendations	14
6 Einige wichtige Hinweise zum Arbeiten mit L^AT_EX	15
6.1 Gliederungen	15
6.2 Referenzen und Verweise	15
6.3 Aufzählungen	15
6.4 Erstellen einer Tabelle	16
6.5 Einbinden einer Grafik	17
6.6 Mathematische Formeln	17
6.7 Weitere nützliche Befehle	18
Bibliography	20
A ESCs analysed	21
B Toolbox instructions	23

Abstract

Hier kommt der Abstact hin ...

Symbols

Symbols

τ	Throttle command
V	Voltage
ω	Angular Speed

Indices

x	x axis
y	y axis

Acronyms and Abbreviations

ETH	Eidgenössische Technische Hochschule
ASL	Autonomous Systems Lab
BLDC	Brush-less Direct Current
PMSM	Permanent Magnet Synchronous Motor
ESC	Electronic Speed Controller
FC	Flight Controller
MAV	Micro Aerial Vehicle
OMAV	Omni-directional Micro Aerial Vehicle
DOF	Degree of Freedom
PWM	Pulse Width Modulation
FOC	Field Oriented Control
EMF	Electro Motive Force
UART	Universal Asynchronous Receiver/Transmitter protocol
UAVCAN	Uncomplicated Application-level Vehicular Communication And Networking
CAN	Controller Area Network

Chapter 1

Introduction

In the past decade, multi-copter type drones have been developed and spread all around the world for applications ranging from geographical mapping to entertainment. Furthermore, the latest developments on Miniature Aerial Vehicles (MAVs) have involved more physical interactions with the environment, power optimization and more Degrees of Freedom (DoFs) which leads to significantly more complex control pipelines. For instance, the Omnidirectional Miniature Aerial Vehicle (OMAV) at the Autonomous Systems Lab (ASL) in ETH Zurich and outlined in [1] consists of 6 pairs of co-axially aligned propellers with tilting axis. Mentioned platform is depicted in Figure 1.1.

Although this novel setup is highly versatile, the current rotor speed control implementation is open-loop, assuming relatively accurate and linear throttle to actual rotor speed mapping. Furthermore, the high number of propellers increases the chance of an individual failure on flight, requiring status information to be sent towards the flight controller (FC). Another important consideration is the aerodynamic interference between coaxial propellers, which surely causes disturbances leading to slower tracking. The extend of this disturbances is still unknown. Therefore, [2] recommends to perform a more thorough identification of this OMAV dynamics to decrease disturbances during optimal control design.

Objectives In this context, this report will describe my work during my semester project with the following objectives:

- Familiarize with current firmware available for FC-ESC communication.
- Achieve rotor speed feedback from the ESC to the FC.



Figure 1.1: ASL OMAV

- Explore different ESC typologies and
- Investigate the characteristics of driving the Brush-less Direct Current (BLDC) motors using an ESC.
- Investigate features available in modern ESCs.

Chapter 2

Literature Review

2.1 Brush-less DC motor driving

2.1.1 Brush-less DC motor

Most UAV platforms spin their propellers using Brushless-DC (BLDC) motors due to their low weight, high top speeds and efficiency. Therefore, it is imperative to know the basic principles to analyze ESCs.

A BLDC motor can be 1, 2 or 3-phase. However, the most efficient version at high speeds and the ones used for UAVs is the 3-phase version. Therefore, the BLDC term will refer to 3-phase BLDC motors. Figure 2.1 shows a simplified diagram with only 4 magnetic poles whereas a typical motor used for UAVs would have 14. Here, the stator includes coils and the rotor has permanent magnets.

2.1.2 BLDC motor driving methods

Two configurations can be used to run BLDC motors as mentioned in [4], both based on Pulse Width Modulation (PWM). These are Trapezoidal and Sinusoidal. They differ in the ideal driving voltage wave-forms to use when driving the motor coils. In both cases, the best performing phase shift between phases is 120° . The effective instantaneous voltage in each coil is a fraction of the DC power supply. PWM approximates this fraction by providing a pulsing signal with a corresponding duty cycle (fraction of time the signal is high). To generate these PWM signals from a DC power source, power MOSFETs are used in bridge configurations. The

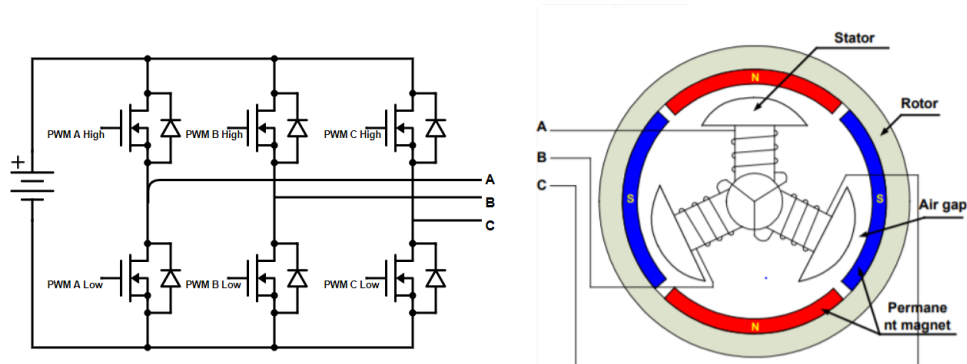


Figure 2.1: *Left* MOSFET bridge driver. *Right* BLDC motor simplified [3]

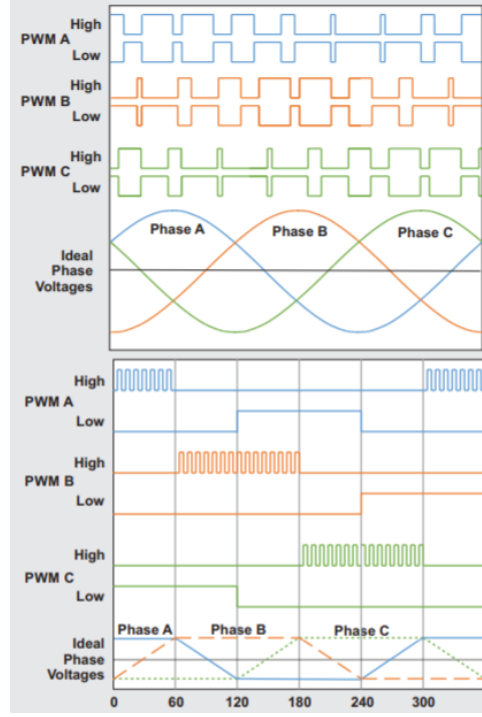


Figure 2.2: PWM Phase signals vs Rotor Position. *Top* Sinusoidal FOC, *Bottom* Trapezoidal. Adapted from [4]

specific configuration used for BLDC motors is shown in Figure 2.1

Trapezoidal: Here the ideal driving waveform is a trapezoidal wave. As shown in Figure 2.2 bottom. This method is easier to implement in hardware since a relatively low accuracy in rotor angular position estimation is needed. However, there are significant power losses caused by many spikes in the signal and also because the electrical magnetic field caused by the stator is only instantaneously at the optimal orientation relative to the rotor magnetic field (perpendicular). Here, the duty cycle put through the active phases is constant for the same rotor speed

Sinusoidal: In this case, the ideal driving waveform is a sinusoid as seen in figure 2.2 top. Note that for the same rotor speed, the duty cycle continuously changes over an electrical period to mimic the ideal sinewave. This is because of the waveform continuously changing and because feedback control ¹ is used to maintain the relative orientation rotor-startor magnetic field orientation optimal (90°). Since the duty cycle is changed more often and depending on the rotor position, this method requires a significantly higher accuracy in rotor angular position estimation. Higher efficiency is obtained in two fronts: less pulsing implies less spikes and therefore switching power losses; the magnetic fields relative orientation is controlled to be optimal.

¹This is not rotor speed control

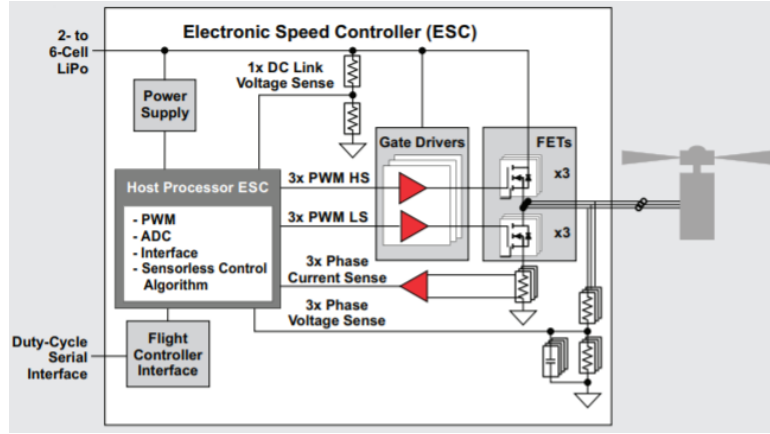


Figure 2.3: ESC general architecture [4]

2.2 Electronic Speed Controllers

2.2.1 General structure

The circuits that run the BLDC motors are commonly known as Electronic Speed Controllers (ESC). However, the majority of current available ones do not perform direct motor speed control. Their core components are a micro-controller, gate drivers, back Electro-motive force (EMF) measurement resistors and the MOSFETs (shown in Figure 2.1). In essence, what they do is receive a throttle signal from a Flight Controller (FC) representing the amplitude of the ideal driving signal (explained in previous subsection, Fig. 2.2). The diagram in Figure 2.3 shows a general electrical architecture of ESCs. Note that gate drivers are simply interface circuits that allow to turn on/off the MOSFETs.

2.2.2 Communications

ESCs need to communicate with the FC to receive throttle commands and in some cases they also send status messages. Hence, some protocols have been used and other have been developed in the context of UAVs.

Analog Protocols

All of these protocols are based on Pulse width modulation given a maximum and a minimum pulse width to be set as maximum and minimum throttle. Hence, these protocols are commonly called RCPWM. The different protocols in this category merely differ in the pulse period. Figure 2.4 depicts these kind of signals on the top and Table 2.1 shows their transmission parameters.

Digital Protocols

Even though most of these protocols are widely known as digital, the true purely digital protocol is UAVCAN. The rest define certain specific pulse time durations to high or low. Dshot will be explained thoroughly in particular given that it's the basis of all the other methods but UAVCAN.

Dshot: This method consists of a 16-bit packet streamed continuously. Each bit is encoded as a pulse with one of two widths, depending on the pulse width version. Figure 2.5 shows the typical DShot signal and the information organization in each packet. The packet is divided into three sections:



Figure 2.4: Oneshot protocol [5]

Table 2.1: ESC protocols' speeds

Protocol	Type	Pulse width range [μs]	Max Update Rate [kHz]
PWM	Analog	1000 - 2000	2000
Oneshot125	Analog	125 - 250	250
Oneshot42	Analog	42 - 84	84
Multishot	Analog	5 - 25	40
Dshot150	Digital	2.5, 5*	9
Dshot300	Digital	1.25, 2.5*	18
Dshot600	Digital	0.625, 1.25*	37
Dshot1200	Digital	0.312, 0.625*	75
Bidirectional Dshot	Digital	Same as Dshot	Same as Dshot
Proshot	Digital	Same as Dshot	Same as Dshot
UAVCAN	Digital	NA	NA

* Pulses can only take either of the two values (Digital)

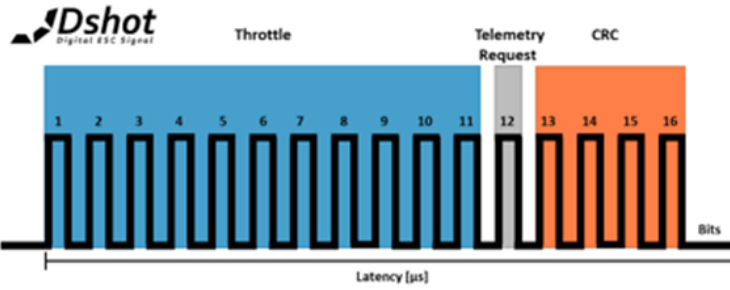


Figure 2.5: Dshot Signal Structure [6]

- Throttle command: Consists of 11 bits (Decimal values 0 -2047). Commands in the range [0,47] are status request commands whereas values in the range [48,2047] encode a 2000 levels throttle command.
- Telemetry request: When this bit is high, telemetry is hight, the ESC is sends a telemetry information packet from the to the FC. Including information such as: Motor Electrical RPM, ESC Temperature, Supply Voltage, Current (Available only in certain ESCs). This telemetry message is sent via another pin using Universal Asynchronous Receiver/Transmitter protocol (UART) at 115200 baudrate.
- Cyclic Redundancy Check (CRC): Used to check for data corruption during transmission.

Bidirectional Dshot: This protocol uses exactly the same signal from the ESC to the FC. The difference is the medium of transfer for the Telemetry signal. In this case, the telemetry packet is sent to the FC through the same throttle pin.

Proshot: The data side of this protocol works the same way as Dshot. The 16 bit digital signal is set as a 4 pulse train where each pulse can encode 4 pulse widths (as opposed to only 2 in Dshot).

UAVCAN: As its name suggests, this a full level software platform based on the Controller Area Network (CAN) bus. It supports two-way communication between multiple agents over a twisted pair wire. The signals sent are merely digital (Only high and low voltages at same duration). The protocol packet convention is illustrated in Figure 2.6. Where the elements are explained in [7] as:

- SOF (1 bit): Dominant Start of Frame bit. Used for synchronization.
- Identifier (11-bits): Establishes message priority.
- RTR (1 bit): Remote Transmission Request. Asks next node for transmission.
- IDE (1 bit): Identifies if standard CAN is used or not.
- r0 (1 bit): Reserved.
- DLC (4 bits): Data length. Number of bytes transmitted.
- Data (1-64 bits): Actual data transmitted.
- CRC (16 bits): Cyclic redundancy check.
- ACK (1 bit): Indicates error free reception.



Figure 2.6: CAN bus protocol [7]

- EOF (7 bits): Indicates end of packet.
- IFS (7 bits): Time required to buffer data.

Hence, communication in this protocol is very reliable on the expense of having to send many extra bits for agent coordination and error checking. The maximum bitrate allowed in this protocol is 1Mbit/s . However, its data transfer rate is decreased by the number of agents connected together and the amount of data each sends. If only one ESC was connected with the FC, the absolute maximum theoretical data rate would be 4.3kHz . Another problem that could arise when using this protocol is significant delays between each rotor command especially between the first motor and the last motor to receive commands. This is because each agent needs to queue when receiving and sending messages as the bus is shared.

2.3 Related Work on ESCs characterization

There have been some studies regarding modeling and characterization BLDC motors driving hardware, given the popularity of their use in UAVs in the last decade. There have been studies in both efficiency and estimation modeling for their dynamic behavior.

2.3.1 Efficiency

Regarding efficiency estimation, several power loss models have been developed based on non-ideal electronic components in the ESCs. Indeed, [8, 9] propose linear and non-linear models for ESC efficiency. There, it is shown that the efficiency changes depending on voltage powering the ESC and current provided to the motor. Furthermore, [10, 11] define complete models of power loss calculation for ESCs driving BLDC motors and [12] models MOSFET power losses. These factors were accounted for in a more generalized model described in [13] and summarized in Equation 2.1.

$$P_{loss} = R_{eq}I_o^2 + (\alpha I_o + \beta)V_{bus} + C f_{eq} V_{bus}^2. \quad (2.1)$$

In this equation, R_{eq} represents the MOSFET on resistance usually given in data-sheets, I_o the output current, V_{bus} the battery voltage, α and β are model values and $C f_{eq}$ is the equivalent capacitance frequency product for overall circuit.

2.3.2 Modeling for Control

Another stream of research is dedicated to determine the input-output characteristics of ESC-BLDC motor behavior.

Direct Throttle to Thrust mapping is subject of investigation by many sources. A linear first order differential relationship about operating points is proposed by [14], with only two determined parameters: gain and time constant. This model was further improved by [15] by introducing a dead-time parameter to account for

communication delays and buffer timing which makes it non-linear. Supply Voltage is shown as another parameter that affects ESC-Throttle mapping in [16] where they define a linear MIMO representation with voltage and throttle as inputs; and current and thrust as output, including non-linear elements.

Other studies have instead focused on the Throttle - rotor speed correspondence. In this category, [17] encountered non-linear steady state mapping. Furthermore, one of the first models that incorporated voltage is given by [18] where the steady state value is defined rotor speed is defined as proportional to the voltage and a first order polynomial of the throttle value, and the dynamics still as a first order differential function, these relationships are detailed in Equations 2.2.

$$\frac{\omega}{V} = at + b \quad \text{and} \quad \frac{\omega/V}{t} = \frac{k}{\tau s + 1}. \quad (2.2)$$

Where a and b are linear fit parameters based on linear fit of steady state data, k and τ are gain and time constant. ω represents rotor speed, V battery voltage and t throttle signal.

Another stream of investigation in this area focused on frequency methods to identify the responses to throttle commands. Chirp sinusoid input throttle signals are used in [19] and the rotor speed output is analyzed. They define a first order differential relation for the ESC output voltage and the utilize a sophisticated motor model to transfer as a transfer function between effective voltage on the motor and rotor speed. Their model even includes cogging modeling, specially important at low speeds. Their complete model is third order differential. Besides, [20] uses steady state response and frequency response using staircase and sinusoidal chirp input throttle signals, but analyses the thrust and torque generated. The model is semi-empirical and includes non-linearities such as torque friction, drag and rotor inertia. However, it assumes a PI loop in the ESC to purpose a model, which is not always the case.

The last stream of investigation in this domain, was merely as data analysis. This includes [21] who analyzed thrust, rotor speed and power outputs, which were presented graphically. Additionally [22] also shows graphical representations of efficiency, power, current, voltage, thrust and torque for different thrust inputs.

Chapter 3

Experimental Setup

3.1 Equipment

3.1.1 ESC Assessment

The most important component for the analysis in this project is the ESC. Therefore, a thorough assessment of different ESCs and their firmware was made. The criteria to pick the particular board took into account that it is to be used with the Voliro OMAV at the ASL in t ETH Zurich depicted in Figure 1.1. The parameters accounted for as well as the top rated ESCs are shown in Table 3.1. Further analyzed ESCs are show in Appendix A.

Therefore, we can see that there are two trends of high-performance ESCs. The first one relates to the most modern ESCs used in drone racing. They are very similar since they are mostly manufactured to use the BlHeli_32 firmware. This firmware, allows for multiple parameter modification via the software BlHeliSuite (see Appendix C for instructions). Given their modularity, they can be made into very small boards. For instance, they now come in 4 in 1 boards (i.e. one board includes 4 ESCs). The other group of high-performing ESCs use UAVCAN as communication protocol with the FC. This gives the advantage of less cabling. They use FOC which makes them more efficient than Sine Modulation versions specially at low rotor speed (below 1000 RPM). These also have possibility of on-board speed control, but it does not include any feed-forward prior. The Holybro Tekko32 F3 ESC was then selected for investigation due to the wide variety of protocols it supports, it's multiple rotor support, good heat-sinking and flexibility to change parameters. Please refer to Section 2.2.2 for a more thorough description of Dshot, Bidirectional Dshot and UAVCAN protocols.

Table 3.1: ESC protocols' speeds

ESC Model	Speed feedback	Brake	Size [mm]	Motors	Protocol	Current Sens	Firmware	Efficiency
Flycolor X-Cross 4in1	Telemetry	Yes	42x45x7.5	4	Dshot	Telemetry	BlHeli_32	Sine Mod
Lumenier Elite 4in1	Telemetry	Yes	43x46x7.5	4	Dshot	Telemetry	BlHeli_32	Sine Mod
Holybro Tekko32 F3 Metal	Telemetry	Yes	42x42x4	4	Dshot	Analog	BlHeli_32	Sine Mod
Myxa by Zubax	UAVCAN	Yes	57x38x24	1	UAVCAN	UAVCAN	Sapog v2	FOC
Holybro Koleta20	UAVCAN	Yes	40x27x5	1	UAVCAN	UAVCAN	Sapog v2	FOC

NOTE: All ESCs that support Dshot in this table support all analog protocols and Bidirectional Dshot

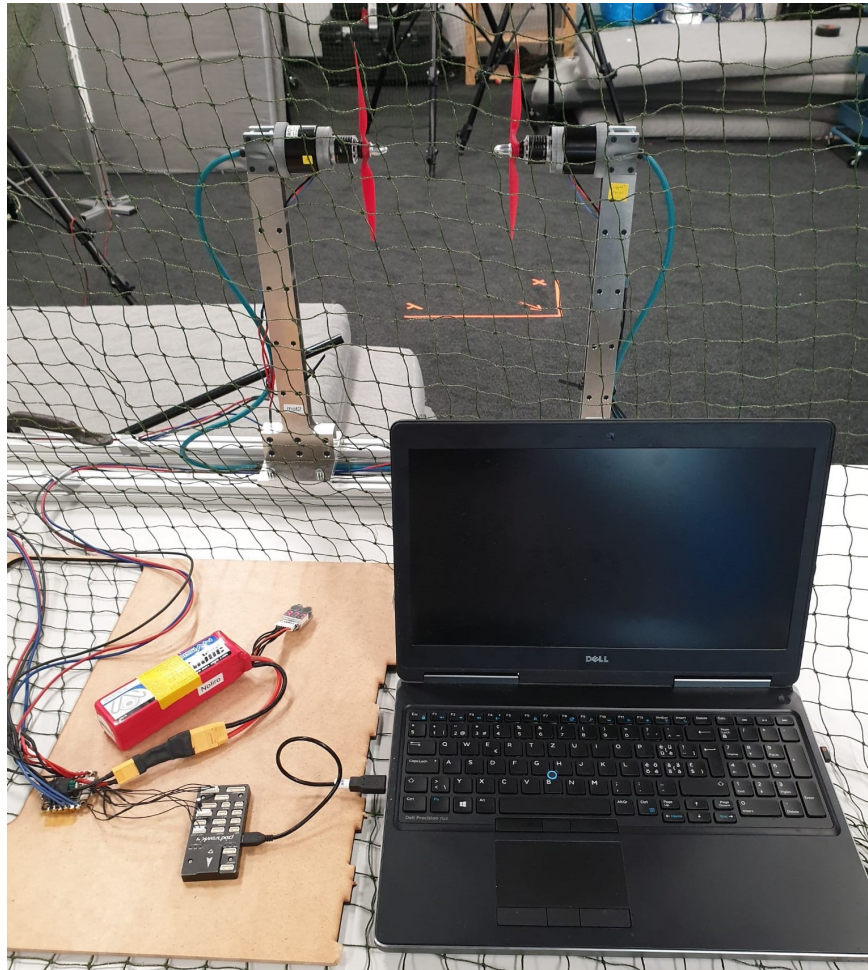


Figure 3.1: Experimental setup

3.1.2 Overall setup

The rig shown in Figure 3.1 was setup for testing purposes and included the following core components:

- 2 BLDC motors by KDE Direct model 2315XF-885Kv 14 poles.
- 1 clockwise Hobbyking Propeller 9in diameter 4.7in pitch.
- 1 counter-clockwise Hobbyking Propeller 9in diameter 4.7in pitch.
- 1 Tekko32 F3 Metal ESC.
- 1 6S LiPo battery.
- Pixhawk 4 flight controller
- Laptop (running Ubuntu 18.04 for firmware compilation).
- Support towers to attach motors.

3.2 Software toolboxes

3.3 Software developed

Chapter 4

ESC charaterization

Chapter 5

Conclusions and Recommendations

Chapter 6

Einige wichtige Hinweise zum Arbeiten mit LATEX

Nachfolgend wird die Codierung einiger oft verwendeten Elemente kurz beschrieben. Das Einbinden von Bildern ist in LATEX nicht ganz unproblematisch und hängt auch stark vom verwendeten Compiler ab. Typisches Format für Bilder in LATEX ist EPS¹ oder PDF².

6.1 Gliederungen

Ein Text kann mit den Befehlen `\chapter{.}`, `\section{.}`, `\subsection{.}` und `\subsubsection{.}` gegliedert werden.

6.2 Referenzen und Verweise

Literaturreferenzen werden mit dem Befehl `\citet{.}` und `\citep{.}` erzeugt. Beispiele: ein Buch [23], ein Buch und ein Journal Paper [23, 24], ein Konferenz Paper mit Erwähnung des Autors: Pratt and Williamson [25].

Zur Erzeugung von Fussnoten wird der Befehl `\footnote{.}` verwendet. Auch hier ein Beispiel³.

Querverweise im Text werden mit `\label{.}` verankert und mit `\cref{.}` erzeugt. Beispiel einer Referenz auf das zweite Kapitel: chapter 6.

6.3 Aufzählungen

Folgendes Beispiel einer Aufzählung ohne Numerierung,

- Punkt 1
- Punkt 2

wurde erzeugt mit:

```
\begin{itemize}
  \item Punkt 1
  \item Punkt 2
\end{itemize}
```

¹Encapsulated Postscript

²Portable Document Format

³Bla bla.

Folgendes Beispiel einer Aufzählung mit Numerierung,

1. Punkt 1

2. Punkt 2

wurde erzeugt mit:

```
\begin{enumerate}
    \item Punkt 1
    \item Punkt 2
\end{enumerate}
```

Folgendes Beispiel einer Auflistung,

P1 Punkt 1

P2 Punkt 2

wurde erzeugt mit:

```
\begin{description}
    \item[P1] Punkt 1
    \item[P2] Punkt 2
\end{description}
```

6.4 Erstellen einer Tabelle

Ein Beispiel einer Tabelle:

Table 6.1: Daten der Fahrzyklen ECE, EU DC, NEFZ.

Kennzahl	Einheit	ECE	EU DC	NEFZ
Dauer	s	780	400	1180
Distanz	km	4.052	6.955	11.007
Durchschnittsgeschwindigkeit	km/h	18.7	62.6	33.6
Leerlaufanteil	%	36	10	27

Die Tabelle wurde erzeugt mit:

```
\begin{table}[h]
\begin{center}
\caption{Daten der Fahrzyklen ECE, EU DC, NEFZ.}\vspace{1ex}
\label{tab:tabnefz}
\begin{tabular}{ll|ccc}
\hline
Kennzahl & Einheit & ECE & EU DC & NEFZ \\
\hline
Dauer & s & 780 & 400 & 1180 \\
Distanz & km & 4.052 & 6.955 & 11.007 \\
Durchschnittsgeschwindigkeit & km/h & 18.7 & 62.6 & 33.6 \\
Leerlaufanteil & \% & 36 & 10 & 27 \\
\hline
\end{tabular}
\end{center}
\end{table}
```

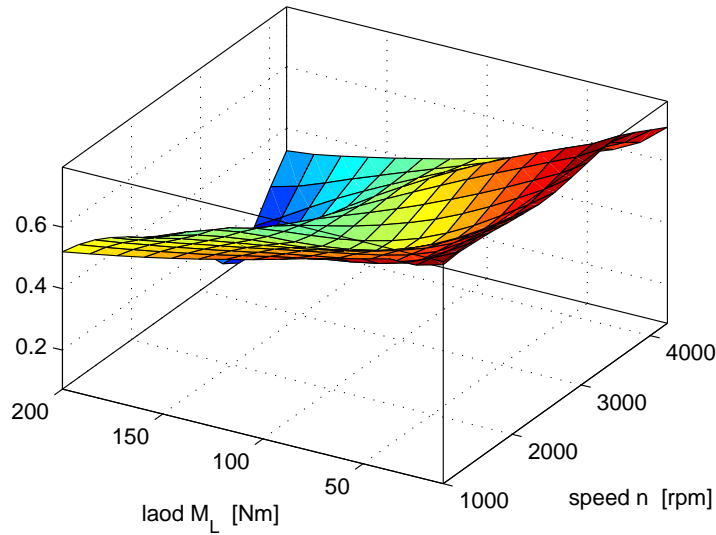


Figure 6.1: Ein Bild

6.5 Einbinden einer Grafik

Das Einbinden von Graphiken kann wie folgt bewerkstelligt werden:

```
\begin{figure}
    \centering
    \includegraphics[width=0.75\textwidth]{images/k_surf.pdf}
    \caption{Ein Bild.}
    \label{fig:k_surf}
\end{figure}
```

oder bei zwei Bildern nebeneinander mit:

```
\begin{figure}
    \begin{minipage}[t]{0.48\textwidth}
        \includegraphics[width = \textwidth]{images/cycle_we.pdf}
    \end{minipage}
    \hfill
    \begin{minipage}[t]{0.48\textwidth}
        \includegraphics[width = \textwidth]{images/cycle_ml.pdf}
    \end{minipage}
    \caption{Zwei Bilder nebeneinander.}
    \label{pics:cycle}
\end{figure}
```

6.6 Mathematische Formeln

Einfache mathematische Formeln werden mit der equation-Umgebung erzeugt:

$$p_{me0f}(T_e, \omega_e) = k_1(T_e) \cdot (k_2 + k_3 S^2 \omega_e^2) \cdot \Pi_{\max} \cdot \sqrt{\frac{k_4}{B}}. \quad (6.1)$$

Der Code dazu lautet:

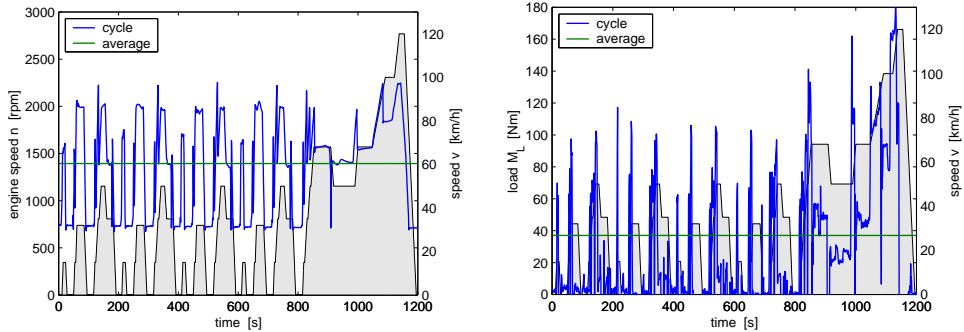


Figure 6.2: Zwei Bilder nebeneinander

```
\begin{equation}
p_{\text{me0f}}(T_e, \omega_e) = k_1(T_e) \cdot (k_2+k_3 S^2 \\
\omega_e^2) \cdot \Pi_{\max} \cdot \sqrt{\frac{k_4}{B}}, .
\end{equation}
```

Mathematische Ausdrücke im Text werden mit `$formel$` erzeugt (z.B.: $a^2+b^2=c^2$). Vektoren und Matrizen werden mit den Befehlen `\vec{.}` und `\mat{.}` erzeugt (z.B. \mathbf{v} , \mathbf{M}).

6.7 Weitere nützliche Befehle

Hervorhebungen im Text sehen so aus: *hervorgehoben*. Erzeugt werden sie mit dem `\textbf{epmh}{.}` Befehl.

Einheiten werden mit den Befehlen `\unit[1]{m}` (z.B. 1 m) und `\unitfrac[1]{m}{s}` (z.B. 1 m/s) gesetzt.

Bibliography

- [1] K. Bodie, Z. Taylor, M. Kamel, and R. Siegwart, “Towards Efficient Full Pose Omnidirectionality with Overactuated MAVs,” in *Proceedings of the 2018 International Symposium on Experimental Robotics*, J. Xiao, T. Kröger, and O. Khatib, Eds. Cham: Springer International Publishing, 2020, pp. 85–95.
- [2] M. Allenspach, K. Bodie, M. Brunner, L. Rinsoz, Z. Taylor, M. Kamel, R. Siegwart, and J. Nieto, “Design and optimal control of a tiltrotor micro aerial vehicle for efficient omnidirectional flight,” 2020.
- [3] J. Zhao and Y. Yu, “Brushless DC Motor Fundamentals,” Monolithic Power Systems, Tech. Rep., 2011.
- [4] K. Mogensen, “Motor-control considerations for electronic speed control in drones,” *Analog Applications Journal*, pp. 1–7, 2016.
- [5] Backyard Robotics, “On ESC Protocols Part II,” 2018.
- [6] Speedgoat, “Dshot usage notes,” 2020.
- [7] S. Corrigan, “Introduction to the Controller Area Network (CAN),” Texas Instruments, Tech. Rep., 2016.
- [8] A. Gong and D. Verstraete, “Experimental testing of electronic speed controllers for UAVs,” in *53rd AIAA/SAE/ASEE Joint Propulsion Conference, 2017*, 2017.
- [9] A. Gong, R. Macneill, and D. Verstraete, “Performance Testing and Modeling of a Brushless DC Motor, Electronic Speed Controller and Propeller for a Small UAV Application,” 2018.
- [10] P. Millett, “Calculating Motor Driver Power Dissipation,” Texas Instruments, Dallas, Texas, Tech. Rep., 2012.
- [11] A. Keskar, N. and Batello, M. and Guerra, A. and Gorgerino, “Application Note AN-1048: Power Loss Estimation in BLDC Motor Drives Using iCalc,” International Rectifier, Tech. Rep.
- [12] M. Graovac, Dušan and Pürschel, “MOSFET Power losses Calculation Using the Data-sheet Parameters,” Infineon, Neubiberg, Germany, Tech. Rep., 2006.
- [13] Tritium, “WaveSculptor 22 Motor Drive User’s Manual,” Tritium, Tech. Rep., 2013.
- [14] M. Yoon, “Experimental Identification of Thrust Dynamics for a Multi-Rotor Helicopter,” *International Journal of Engineering Research & Technology (IJERT)*, vol. 4, no. 11, pp. 206–209, 2015.

- [15] R. T. Torres and F. Sergii, “Brushless Direct Current Propulsion System Identification,” in *Integrated Computer Technologies in Mechanical Engineering*, M. Nechyporuk, V. Pavlikov, and D. Kristskiy, Eds. Cham: Springer International Publishing, 2020, pp. 105–113.
- [16] G. Szafranski, R. Czyba, and M. BŁachuta, “Modeling and identification of electric propulsion system for multirotor unmanned aerial vehicle design,” in *2014 International Conference on Unmanned Aircraft Systems (ICUAS)*, 2014, pp. 470–476.
- [17] J. A. Prakosa, D. V. Samokhvalov, G. R. V. Ponce, and F. Sh. Al-Mahturi, “Speed Control of Brushless DC Motor for Quad Copter Drone Ground Test,” in *2019 IEEE Conference of Russian Young Researchers in Electrical and Electronic Engineering (EICONRUS)*, 2019, pp. 644–648.
- [18] A. Moutinho, E. Mateos, and F. Cunha, “The Tilt-Quadrotor: Concept, Modeling and Identification,” in *2015 IEEE International Conference on Autonomous Robot Systems and Competitions*, 2015, pp. 156–161.
- [19] C. Xiang, X. Wang, Y. Ma, and B. Xu, “Practical Modeling and Comprehensive System Identification of a BLDC Motor,” *Hidawi Publishing Corporation*, vol. 2015, pp. 1024–123X, 2015.
- [20] L. Wu, Y. Ke, and B. Chen, “Systematic Modeling of Rotor-Driving Dynamics for Small Unmanned Aerial Vehicles,” *Unmanned Systems*, vol. 6, no. 2, pp. 81–93, 2018.
- [21] D. Kotarski, M. Krznař, P. Piljek, and N. Simunic, “Experimental Identification and Characterization of Multirotor {UAV} Propulsion,” *Journal of Physics: Conference Series*, vol. 870, p. 12003, jul 2017.
- [22] M. Sulewski, L. Ambroziak, M. Kondratiuk, and A. Stulgis, “Identification of electric propulsion system for unmanned aerial vehicles,” *AIP Conference Proceedings*, vol. 2029, no. 1, p. 20072, 2018.
- [23] M. Raibert, *Legged Robots That Balance*. Cambridge, MA: MIT Press, 1986.
- [24] M. Vukobratović and B. Borovac, “Zero-moment point — thirty five years of its life,” *International Journal of Humanoid Robotics*, vol. 1, no. 01, pp. 157–173, 2004.
- [25] G. A. Pratt and M. M. Williamson, “Series elastic actuators,” in *IEEE/RSJ International Conference on Intelligent Robots and Systems (IROS)*, 1995, pp. 3137–3181.

Appendix A

ESCs analysed

Table A.1: ESCs analyzed

Model	Source
Flycolor X-Cross 4in1	https://www.getfpv.com/flycolor-x-cross-60a-3-6s-blheli32-4-in-1-esc.html
Lumenier Elite 4in1	https://www.getfpv.com/lumenier-elite-60a-2-6s-blheli-32-4-in-1-esc.html
Diatone Mamba 4in1	https://www.getfpv.com/diatone-mamba-506-50a-6s-dshot1200-4-in-1-esc.html
Hobbywing Xrotor micro 4in1	https://www.getfpv.com/hobbywing-xrotor-micro-60a-6s-4-in-1-blheli32-esc.html
T-Motor F55A Pro II	http://store-en.tmotor.com/goods.php?id=766
Aikon AK32	https://fpvracing.ch/de/esc/2762-aikon-ak32-blheli32-55a-4in1-esc-3-6s.html
Holybro Tekko32 F3	https://fpvracing.ch/de/esc/2598-holybro-tekko32-f3-metal-4in1-esc-4-6s.html
Myxa by Zubax	https://zubax.com/products/myxa?gclid=Cj0KCQjwgJv4BRCrARIsAB17JI6NbuRoO7aqXnWGHVKWznI7bw07vGcZHrsc7aJW299Lf9puqg4C_V0aAiHGEALw_wcB
Holybro Koleta20	http://www.holybro.com/product/kotleta20/
KISS ESC32A	https://kiss.flyduino.net/the-kiss-experience/kiss-esc32a-32bit-electronic-speed-controller/
DJI TAKYON Z650/Z660	https://www.dji.com/ch/takyon-z650?site=brandsitefrom=landing_page
DJI TAKYON Z425-M/Z415-M	https://www.dji.com/ch/takyon-z425-m-and-z415-m?site=brandsitefrom=landing_page
Foxtech 8120 FOC	https://www.foxtechfpv.com/foxtech-8120-100kv-foc-esc-hv-combo-2.html#yt_tab_products1
X2-series TMM 6026-3	https://www.mgm-controllers.com/helicopters/speed-controllers-escs-3/tmm-6026-3-for-helicopters-x2-series.html
T-Motor ALPHA 40A	http://store-en.tmotor.com/goods.php?id=580
T-Motor FLAME 60A HV	http://store-en.tmotor.com/goods.php?id=370
T-Motor AT 30A	http://store-en.tmotor.com/goods.php?id=901

Appendix B

Toolbox instructions

Appendix C

BlHeli Suite Instructions